ACS APPLIED MATERIALS & INTERFACES

Research Article

www.acsami.org

Novel Hierarchically Porous Carbon Materials Obtained from Natural Biopolymer as Host Matrixes for Lithium–Sulfur Battery Applications

Bin Zhang,[†] Min Xiao,[†] Shuanjin Wang,*[,†] Dongmei Han,[†] Shuqin Song,[†] Guohua Chen,[‡] and Yuezhong Meng*[,†]

[†]The Key Laboratory of Low-carbon Chemistry & Energy Conservation of Guangdong Province/State Key Laboratory of Optoelectronic Materials and Technologies, Sun Yat-sen University, Guangzhou 510275, P. R. China

[‡]Department of Chemical Engineering, Hong Kong University of Science & Technology, Hong Kong, P. R. China

ABSTRACT: Novel hierarchically porous carbon materials with very high surface areas, large pore volumes and high electron conductivities were prepared from silk cocoon by carbonization with KOH activation. The prepared novel porous carbon-encapsulated sulfur composites were fabricated by a simple melting process and used as cathodes for lithium sulfur batteries. Because of the large surface area and hierarchically porous structure of the carbon material, soluble polysulfide intermediates can be trapped within the cathode and the volume expansion can be alleviated effectively. Moreover, the electron transport properties of the carbon materials can provide an electron conductive network and promote the utilization rate of sulfur in cathode. The prepared carbon–sulfur composite exhibited a high specific capacity and excellent cycle stability. The results show a high initial discharge capacity of 1443 mAh g^{-1} and retain 804 mAh g^{-1} after 80 discharge/charge cycles at a rate of 0.5 C. A Coulombic efficiency retained up to 92% after 80 cycles. The prepared hierarchically porous carbon materials were proven to be an effective host matrix for sulfur encapsulation to improve the sulfur utilization rate and restrain the dissolution of polysulfides into lithium–sulfur battery electrolytes.

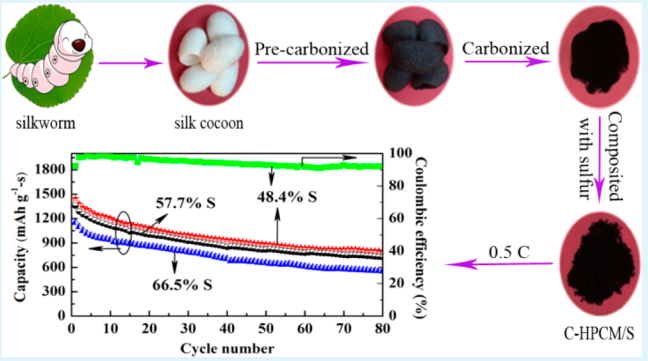

KEYWORDS: *hierarchically porous carbon materials, biopolymers, carbon–sulfur composites, cyclical stability, electron conductivity, lithium–sulfur batteries*

INTRODUCTION

With the urgent needs of energy storage for portable electronics, hybrid electric vehicles, and large industrial equipment, more and more attentions have been paid to the development of Li-ion batteries.[1−5] However, the current Li-ion batteries will no longer satisfy the requirements of the future electric vehicles because of the low inherent capacity of the conventional cathode materials, such as ∼148 mAh g^{-1} for $LiMn_2O_4$, ∼170 mAh g^{-1} for $LiFePO_4$ and ∼274 mAh g^{-1} for $LiCoO_2$.[6−9] Nowadays, the energy density of Li-ion batteries has approached their ceilings. Hence, researchers have currently moved their interests to developing novel cathode materials with higher gravimetric and volumetric capacities.

Lithium–sulfur (Li–S) batteries have attracted researchers' extensive attention for more than two decades because of a high theoretical specific capacity (1675 mAh g^{-1}) and a high theoretical energy density (2600 Wh kg^{-1}), which are 3–5 fold higher than those of state-of-art Li-ion batteries.[9−11] The abundance of sulfur in nature makes it a cheap material, which reduces the cost of Li–S batteries.[12,13] Despite these significant advantages, there are several problems and challenges that have to be solved for Li–S batteries, such as the low electron conductivity of sulfur and its reduced products, the dissolution and diffusion of polysulfide intermediates, and the volume expansion of sulfur intermediates during cycling.[14−17] The poor electron conductivity of sulfur directly leads to the low electrochemical utilization rate of sulfur. The obvious volumetric expansion of sulfur cathode during the charge–discharge process can be described by the reaction S + 2Li → Li_2S. The reason is the density of Li_2S (1.66 g cm^{-3}) is lower than that of sulfur (2.03 g cm^{-3}).[6] The volumetric expansion of sulfur cathode may cause the instability of cathode structure. Additionally, different from conventional lithium-ion batteries that operate on the basis of topotactic intercalation reactions, the charge–discharge process of sulfur with a metallic lithium anode involves two-electron-transfer electrochemical reaction, and forms a series of polysulfide intermediates.[18,19] The dissolution and shutting effect of the polysulfide intermediates results in poor cyclical stability, severe lithium anode corrosion and low Coulombic efficiency.[19,20] To address these challenges, a great deal of effort has been made, such as finding a suitable host matrix for sulfur encapsulation, to enhance the electron

Received: May 18, 2014
Accepted: July 15, 2014
Published: July 15, 2014

Scheme 1. Schematic of Preparation Process for C-HPCM/S Composites

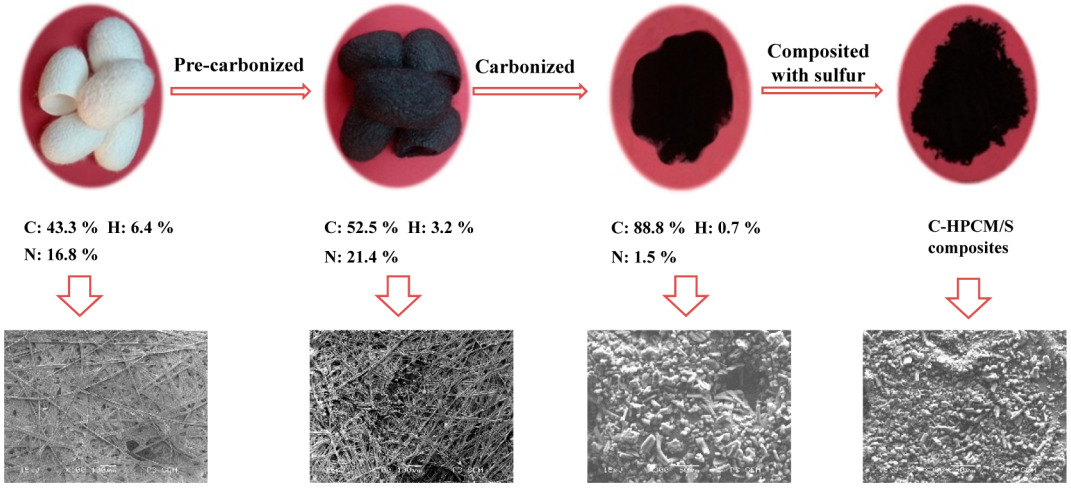

conductivity of the cathode as well as hinder polysulfide diffusion. There are two methods to improve the performance of sulfur cathode. One is fixing sulfur onto the polymer chains via covalent bond to obtain a kind of rich-sulfur organic substance by chemical reactions.[21,22] The other is coating or encapsulating sulfur in host matrixes, such as conductive polymers (polypyrrole, polyaniline, polythiophene, etc.),[23−25] porous carbon materials (mesoporous carbons, graphene oxides, carbon nanotubes et al.) and graphene.[26−28] These polymer−sulfur and carbon−sulfur composites have helped to improve utilization rate of sulfur and cycling stability. Among the above researches, porous carbon materials are particularly attractive due to their excellent electron conductivity and inherently large surface area. Their excellent electron conductivities lead to a high utilization rate of active materials. Their large surface area, porous structure and strong adsorption ability are responsible for minimizing or avoiding dissolution and the shuttle of polysulfides.[20] Notable successes were implemented by Nazar et al., who pioneered the developments of mesoporous carbons for sulfur encapsulation, and achieved a very high specific capacity of around 1300 mAh g^{-1}.[14] Stefan Kaskel's group prepared a kind of mesoporous carbon materials called Kroll-Carbons with specific surface area ranging close to 2000 m^2 g^{-1}. The Kroll-Carbons showed outstanding performance as cathodes in lithium−sulfur batteries. The coin cell assembled by them showed initial specific capacity of near to 1400 mAh g^{-1}.[29] In these porous carbon encapsulated sulfur composites, the surface areas and electron conductivities of the host matrixes are very important for the electrochemical performance of the cathode.

Silk cocoon is one of an abundant biopolymer in nature. It has been used to prepare porous carbon materials by carbonization. The carbonization process of silk cocoon is an important way for obtaining porous carbon materials with high BET surface area. Liang Y. R. et al.[30] prepared 1D hierarchically porous carbon microfibers (HPCMFs) from silk cocoon with porous structure, which exhibited the BET surface area of 796 m^2 g^{-1}. Jin H. J. et al.[31] fabricated novel carbon based microporous nanoplates containing numerous heteroatoms (H-CMNs) from the regenerated silk fibroin and found that a high surface was induced by carbonization with KOH activation. The prepared H-CMNs possessed a high BET surface area up to 2557 m^2 g^{-1}. These porous carbon materials (C-PCMs) from silk cocoon biopolymer have been used as supercapacitor electrodes and presented superior electrochemical performance.[31] To the best of our knowledge, there is no report on the application of C-PCMs as host matrixes for Li−S batteries.

In this work, we employed a simple method to prepare hierarchically porous carbon materials (C-HPCMs) from silk cocoon biopolymer, and explored the possibility using them as host matrixes for lithium−sulfur battery cathode materials. The prepared C-HPCMs possess super high surface area of 3243 m^2 g^{-1}, hierarchical structure with large pore volume of 2.1 cm^3 g^{-1}, and excellent electron conductivity (1.0 S cm^{-1}). The C-HPCM encapsulating sulfur composites (C-HPCM/S) were prepared by simple melting diffusion method. The electrochemical properties of C-HPCM/S composite cathode exhibit an initial discharge capacity of 1443 mAh g^{-1} and remain a capacity of 804 mAh g^{-1} after 80 cycles at a rate of 0.5 C.

EXPERIMENTAL SECTION

Preparation of Hierarchically Porous Carbon Materials (C-HPCMs) from Silk Cocoon. Silk cocoons were cleaned using deionized water and dried at 40 °C in the oven for 24 h. The dried silk cocoons were precarbonized at 350 °C for 2 h with a heating rate of 1 °C min^{-1}. And then grinded with KOH (w/w = 1:0.5, 1:1, and 1:1.5) together. The mixtures were calcined at 900 °C for 1 h with a heating rate of 3 °C min^{-1} under N_2 atmosphere in a tubular furnace. The obtained carbon materials were treated with 1 M HNO_3 three times (3 h for each time), washed with deionized water and dried at 100 °C for 24 h in a vacuum oven.

Preparation of C-HPCM Encapsulating Sulfur Composites (C-HPCM/S). The C-HPCM/S composites were prepared by following a conventional melting diffusion strategy. The as-prepared C-HPCMs and sublimed sulfur with different weight ratios (C-HPCMs: S = 1:1, 2:3, and 3:7) were grinded together, transferred to a tubular furnace, and heated at 155 °C for 6 h with a heating rate of 3 °C min^{-1} under a N_2 atmosphere. After cooling down to room temperature, the C-HPCM/S composites were obtained and sealed in the glass bottles prior to use.

Materials Characterization. Thermogravimetric analysis (TGA) was conducted on PerkinElmer Pyris Diamond thermogravimertic/differential thermol analyzer. Nitrogen adsorption−desorption isotherms and pore size distribution were characterized by accelerated surface area and porosimetry system (Micromeritics, ASAP 2010). Elemental analysis (EA) was performed on Elementar Vario EL Cube elemental analyzer. The X-ray diffraction (XRD) was conducted by an X'Pert Pro diffractometer using Cu Kα radiation (λ = 0.15418 nm). The morphology was characterized by scanning electron microscopy (SEM, Hitachi, S4700 and SEM, JEOL JSM model 820). Electron

conductivity was measured on a semiconductor powder electron conductivity test board (Suzhou Jinge Electronic Co., Ltd., SZT-D).

Electrochemical Characterization. Cathodes from the C-HPCM/S composite were prepared by a slurry coating procedure. The cathode slurry consisted of 70 wt % the as-prepared C-HPCM/S composite, 20 wt % carbon black (Super P Conductive Carbon Black) and 10 wt % polyvinylidene fluoride (PVDF). *N*-methylpyrrolidinone (NMP) was used as the solvent. The slurry was coated onto aluminum foil current collectors and then dried at 60 °C overnight. The electrodes were cut into disks of 10 mm in diameter and the sulfur loading was about 0.2 mg cm^{-2}. CR2025-type coin cells were assembled in an argon-filled glovebox. The electrolyte used was 1 M bis(trifluoromethane) sulfonimide lithium salt (LiTFSI) dissolved in a mixture of 1,3-dioxolane (DOL) and dimethoxymethane (DME) with a volume ration of 1:1, including 0.1 M $LiNiO_3$ as an electrolyte additive. Lithium metal was used as the counter electrode and a microporous polyethylene membrane (Celgard 2400) was used as separator. Galvanostatic charge−discharge tests were performed at different current densities in the potential range of 1.5−2.8 V versus Li/Li^+ using a CT2001A cell test instrument (LAND Electronic Co. Ltd., China). All specific capacity values were calculated on the basis of sulfur mass. Cyclic voltammetry (CV) measurements were performed using a Solartron S1287 electrochemical interface at a scan rate of 0.1 mV s^{-1} in the potential range of 1.0 to 3.0 V versus Li/Li^+. Electrochemical impedance spectroscopy (EIS) was measured in the 1 MHz to 0.1 Hz frequency range with the applied voltage of 5 mV on an electrochemical working station PCI4/300 (Gamry Instrument, Warminster, PA, USA). All the electrochemical tests were performed at room temperature.

RESULTS AND DISCUSSION

Characterization of C-HPCMs and C-HPCM/S Composites. As shown in Scheme 1, C-HPCMs were prepared in two steps. The first step was the precarbonation of silk cocoons at a low temperature of 350 °C. The second step was the final carbonation of the precarbonized product at a high temperature of 900 °C. The high surface area can be induced by KOH activation. The different weight ratios of precarbonized carbon/KOH (1:0.5, 1:1, and 1:1.5) were designed to get C-HPCMs with different surface areas.

N_2 adsorption isotherms were measured to elucidate the BET surface areas and the porous structure of the as prepared C-HPCMs. BET surface area of the C-HPCMs from different ratios of the precarbonized carbon to KOH are as high as 1871, 2181, and 3243 m^2 g^{-1}. The corresponding samples are termed as C-HPCM1800, C-HPCM2100, and C-HPCM3200 in turns. The N_2 adsorption−desorption isotherms curves of C-HPCMs can be identified as type IV in the IUPAC classification with typical H1 hysteresis loop as shown in Figure 1.[29] Taking the curve of C-HPCM3200 as an example, it can be seen that the pore sizes range from micropores to macropores. Specifically, the adsorption uptake at relatively low pressure (P/P_0) also reveals the existence of micropores. The following slope at medium relative pressure and the hysteresis loop illustrates the presence of mesopores, and the final increased tail at relative high pressure from 0.95 to 1.0 (P/P_0) indicates the existence of macropores. As shown in the pore size distribution (PSD) curves of Figure 2, the C-HPCMs showed distinctly hierarchical pores. Three main pore size regions can be found for C-HPCM3200: (1) micropores region in the ranges of 0.4−2.4 nm; (2) mesopores region in ranges of 2.5−40 nm; (3) macropore region in the range of 50−100 nm. The macropores in C-HPCM3200 are much stronger in signal than the macropores in C-HPCM2100 and C-HPCM1800. The C-HPCM3200 has a pore volume of 2.1 cm^3 g^{-1} and an average pore diameter of 2.6 nm. The C-HPCM1800 shows a similar

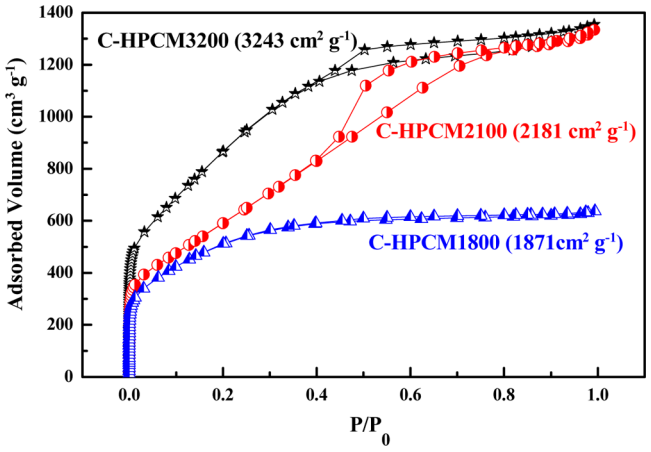

Figure 1. N_2 adsorption−desorption isotherms and specific surface area of C-HPCMs.

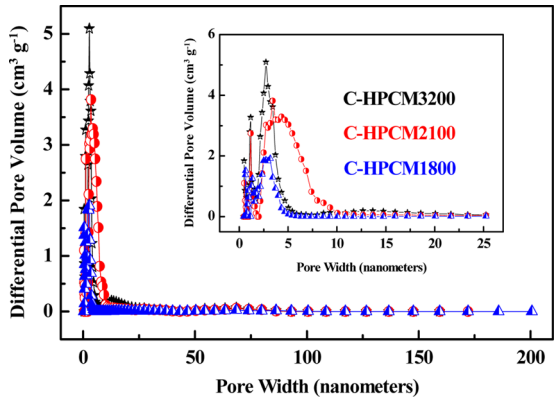

Figure 2. Pore size distribution of C-HPCMs.

pore size distribution with C-HPCM3200, whereas the C-HPCM2100 shows some differences. The C-HPCM2100 has wider mesopores distribution within 2.4−10 nm. The KOH treatment induced formation of hierarchical pores and the high surface area of C-HPCMs. The suggested mechanism is that the activation of carbon with KOH conducts as $6KOH + C \leftrightarrow 2K + 3H_2 + 2K_2CO_3$, followed by decomposition of K_2CO_3 and/or reaction(s) of $K/K_2CO_3/CO_2$ with carbon.[31,32]

Elemental analyses of the C-HPCMs were performed and the results are listed in Table 1. The results show that C-HPCMs

Table 1. Elemental Analysis Results of C-HPCMs

name	C[%]	H[%]	N[%]	C/N ratio
C-HPCM3200	88.8 ± 0.3	0.7 ± 0.3	1.5 ± 0.3	61.2
C-HPCM2100	84.1 ± 0.3	0.5 ± 0.3	5.9 ± 0.3	14.2
C-HPCM1800	77.6 ± 0.3	1.4 ± 0.3	7.6 ± 0.3	10.3

contained a small quantity of nitrogen, indicating that some nitrogen groups in silk cocoon still exists after carbonization. Generally, nitrogen is one of the most attractive elements, which could improve the carbon wettability, adsorption ability, surface polar, and electron conductivity. It has been reported that nitrogen-doping could enhance the reduction of sulfur, and provide high discharge potential and initial discharge capacity.[33] Furthermore, nitrogen-doping could assist the mesoporous carbon to inhibit the diffusion of polysulfide species into the electrolyte by means of the enhanced interface adsorption.[34] In

other words, the presence of nitrogen atom is expected to improve electrochemical performance of C-HPCM/S composite cathodes. The electron conductivity of the host matrix can improve electrochemical activity and utilization rate of sulfur. Before electron conductivity measurements, the powder C-HPCMs were compressed into disks under varying pressure (2, 4, 6, 8, and 10 MPa). It can be seen from Table 2 that the electron conductivity of C-HPCMs increase with the increase of pressure. Meanwhile, C-HPCM3200 and C-HPCM2100 show the better electron conductivities than C-HPCM1800. Considering both specific surface area and electron conductivity of C-HPCMs, C-HPCM3200 was investigated as a host matrix for encapsulation of sulfur to prepare C-HPCM/S composites cathodes.

Table 2. Electron Conductivities of C-HPCMs

	electron conductivity (S cm^{-1})		
pressure (MPa)	C-HPCM3200	C-HPCM2100	C-HPCM1800
2	0.5 ± 0.1	0.6 ± 0.2	0.3 ± 0.1
4	0.7 ± 0.2	1.0 ± 0.2	0.5 ± 0.1
6	1.0 ± 0.1	1.4 ± 0.3	0.6 ± 0.2
8	1.4 ± 0.2	1.8 ± 0.2	0.7 ± 0.1
10	1.6 ± 0.3	2.3 ± 0.1	0.8 ± 0.2

TGA was used to ascertain sulfur contents in C-HPCM/S composites and depicted in Figure 3. TGA curves of sulfur and C-HPCM3200 are shown for easier comparison. A slight weight loss of 8.2 wt % for the origin C-HPCM3200 is found before 450 °C, which ascribe to the desorption of water in the hierarchical pores and decomposition of the containing nitrogen groups in carbon materials This proves that although final carbonization conducts at a very high temperature. Despite this, there are still a few containing nitrogen groups existing in C-HPCMs as shown in Table 1. The adsorbed water in its pores facilitates decomposition of these groups when running TGA test. After subtracting this weight loss, the sulfur contents can be calculated from the reduction in weight of the C-HPCM/S composites. We obtained three samples of C-HPCM3200/S with different sulfur contents, 48.4 wt %, 57.7 and 66.5 wt %, which named as C-HPCM3200-48.4%S, C-HPCM3200-57.7%S and C-HPCM3200-66.5%S in its turns. In addition, the weight loss of sulfur sublimation in C-HPCM3200/S composites is postponed to high temperature compared with element sulfur. It proves that sulfur in C-HPCM3200/S composites was restricted effectively in the pores of C-HPCMs. This is consistent with the results of BET measurements for C-HPCM3200/S composites as follows.

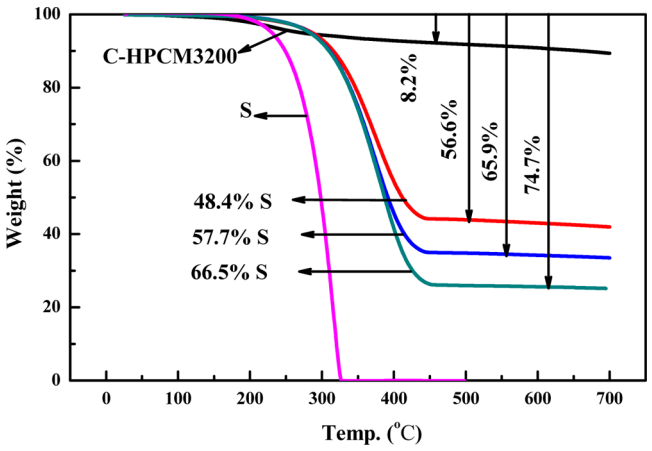

Figure 3. TGA curves of sublimed sulfur, C-HPCM3200, and C-HPCM3200/S composites.

The N_2 adsorption−desorption isotherms and PSD curves of C-HPCM3200/S composites are presented in Figures 4 and 5,

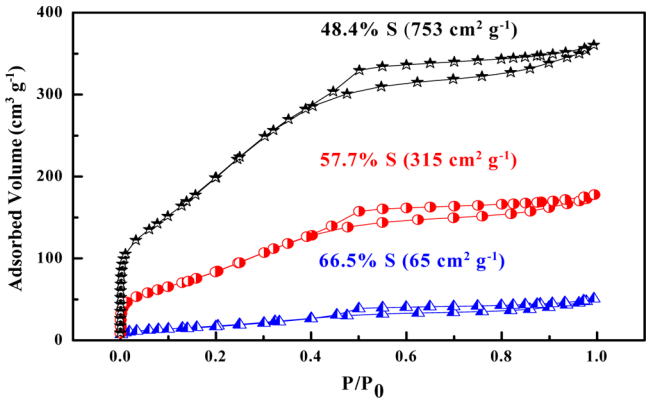

Figure 4. N_2 adsorption−desorption isotherms and specific surface area of C-HPCM3200/S composites with different sulfur contents.

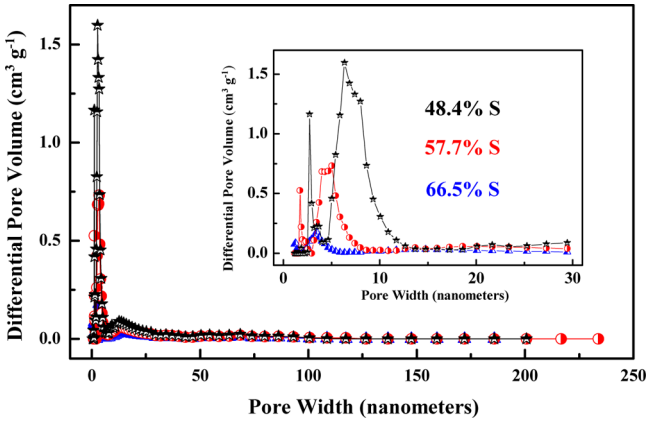

Figure 5. Pore size distributions of C-HPCM3200/S composites with different sulfur contents.

respectively. After the impregnation of sulfur, the specific areas of C-HPCM3200/S composites with different sulfur loading decrease sharply from 3243 to 753, 615, and 65 cm^2 g^{-1}, and their pore volumes decrease from 2.1 to 0.6, 0.3, and 0.1 cm^3 g^{-1} when compared with those of the pristine C-HPCMs. The results indicate that there still remains a volume for sulfur expansion in C-HPCM3200/S composites even after the encapsulation of sulfur. As shown in Figures 2 and 5, C-HPCM3200/S composites exhibit the different pore size distribution compared with its pristine porous carbon. The porous volumes of mesopores (20−40 nm diameter) and macropores (50−100 nm diameter) decrease obviously. Taking C-HPCM3200-66.5%S as an example, its microspores and small mesopores in the range of 0.4−5 nm almost disappear. With the increase in sulfur content, the mesopores with diameters of 20−40 nm disappear finally, whereas the mesopores with diameters of 5−10 nm increase. Furthermore, the mesopores with diameters of 10−40 nm and macropores with diameters of 50−100 nm decrease accordingly. This can be attributed to the diffusion of sulfur into mesopores and then

dx.doi.org/10.1021/am503069j | ACS Appl. Mater. Interfaces 2014, 6, 13174−13182

into macropores, followed by transforming into mesopores, until all the pores were "stuffed".[5]

The X-ray diffraction (XRD) patterns of sublimated sulfur, C-HPCM3200 and C-HPCM3200/S composites are presented in Figure 6. The broad diffraction peaks at around 24° and 44°

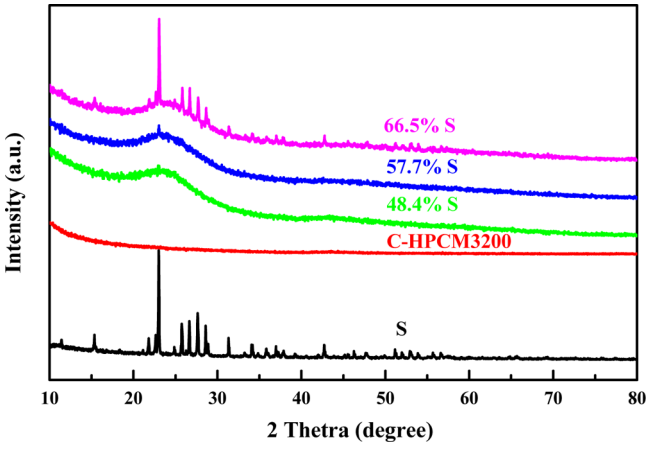

Figure 6. XRD patterns of sublimated sulfur, C-HPCM3200, and C-HPCM3200/S composites.

are for C-HPCM/S composites, corresponding to amorphous characteristics of carbon materials.[19] However, only a broad diffraction peak at around 44° is found for C-HPCM3200, whose broad diffraction peak at around 24° is not observed clearly. This is due to its high amorphous structure. The characteristic peaks of element sulfur cannot be detected for C-HPCM3200-48.4%S and C-HPCM3200-57.7%S composites. These suggests that sulfur successfully diffused into the pores of C-HPCM3200/S composites and existed in a highly dispersed state. This conclusion is also confirmed by SEM observations. The characteristic peaks of sulfur are observed in C-HPCM3200-66.5%S composite, indicating that sulfur crystallized on the outer surface of the C-HPCM3200 after overloading sulfur.

Figure 7 shows the SEM microstructures of silk cocoon, C-HPCM3200 and C-HPCM3200−48.4%S composites. The SEM image in Figure 7a shows that silk cocoon is composed of interlaced 1D silk microfibers with about 10−15 mm in diameter. After a precarbonization treatment at 350 °C, the carbon microfibers in the precarbonized silk cocoon preserve the well-defined fibrous morphology in Figure 7b. The SEM image in Figure 7e demonstrates that the as-prepared carbon microfibers subjected to being ground had homogeneous length (<50 um). It can be seen from Figures 7c and d that C-HPCM3200 exhibit hierarchical pores, including micropores (<5 nm), small mesopores (5−50 nm) and macropores (>50 nm). When sulfur diffused into the pores, most pores disappear and some macropores change into mesopores in C-

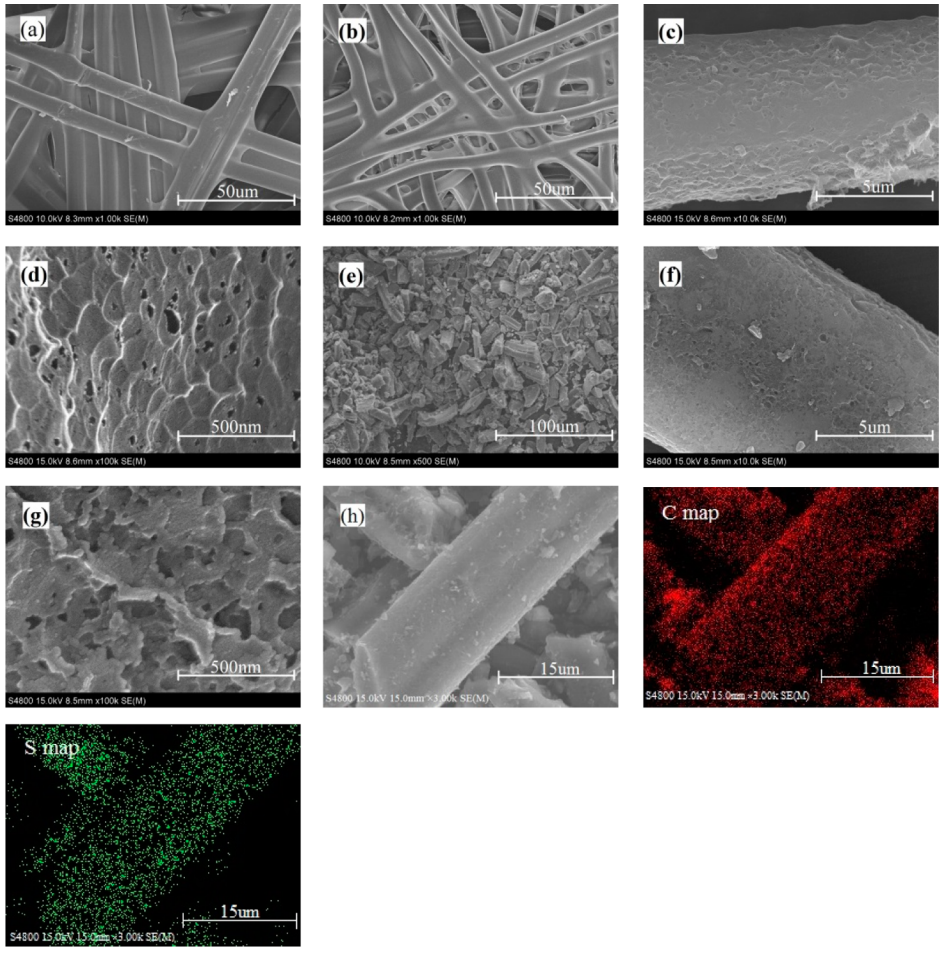

Figure 7. (a, b) SEM images of silk cocoon before and after being precarbonized, (c, d) C-HPCM3200, (e−g) C-HPCM3200-48.4%S. (h) SEM mapping of C-HPCM3200-48.4%S.

HPCM3200/S composite as shown in Figures 7f and g. Elemental X-ray mapping (Figure 7h) shows a homogeneous distribution of sulfur within C-HPCMs matrix. It is apparent that the prepared C-HPCMs with hierarchically porous structure are good host matrixes for encapsulating sulfur. The C-HPCM/S composites cathodes are expected to suppress the dissolution of sulfur into electrolyte and provide considerable cycling stability.

Electrochemical Measurements. The cyclic discharge performance of the C-HPCM3200/S composites cathodes with different sulfur contents at a current rate of 0.5 C (by the weight sulfur, 1C = 1675 mA g^{-1}) between 2.8 and 1.5 V at room temperature are shown in Figure 8. C-HPCM3200/S

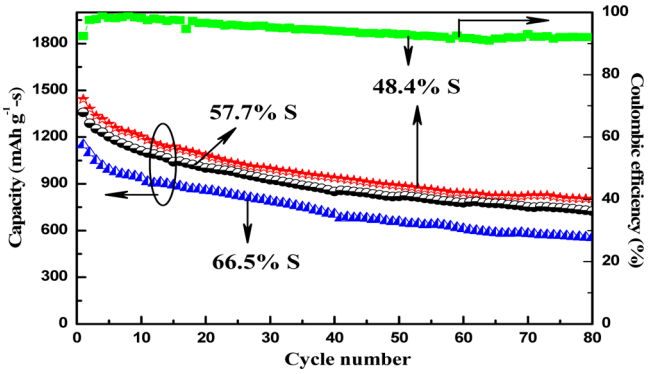

Figure 8. Discharge cyclic performance of C-HPCM3200/S composites with different sulfur contents at a current rate of 0.5 *C*.

composite with 48.4 wt % sulfur content shows very high initial specific capacity of 1443 mAh g^{-1} and kept the specific capacity of 804 mAh g^{-1} after 80 cycles, revealing the highest capacities and the best cycling stability among C-HPC3200/S composites. The comparison of the performance with the data in other published references are tabulated in Table 3. It can be seen

Table 3. Specific Capacity of C-HPCM3200-48.4%S and Data from References

	initial discharge capacity (mAh g^{-1})	discharge capacity after 50 cycles (mAh g^{-1})	capacity retention (%)	sulfur content (%)	ref
1	1443 ± 23	886 ± 11	61 ± 0.2	48.4 ± 0.3	this work
2	1350	709	52	55	20
3	1106	580	52	60	35
4	1305	469	36	75	36
5	1400	650	46	64	37
6	1300	450	35	40	38
7	1285	878	69	57	5
8	1100	730	66	54	19

that the prepared C-HPCM3200/S composite exhibits the highest initial specific capacity and excellent cycle stability. Moreover, C-HPCM3200/S composite with 48.4% sulfur content shows high Coulumbic efficiency over 92% after 80 cycles. Although C-HPCM/S composites with 57.7 and 66.5 wt % of sulfur contents exhibit high initial specific capacities of 1358 and 1150 mAh g^{-1} respectively, their specific capacities decrease faster than C-HPCM3200−48.4%S during cycling test. The high initial specific capacities of these C-HPCM/S composites are believed to be resulted from the good electron conductivity of C-HPCMs host matrixes, which can facilitate the electrochemical reaction of sulfur. Their hierarchal pores provide spaces not only for accommodation of sulfur, but also for volume expansion of sulfur in the charge/discharge process. C-HPCM3200-66.5%S contains a small amount of sulfur on the outer surface of the host matrix. C-HPCM3200−48.4%S still possesses the sufficient pore volume to provide spaces for cathode's volumetric expansion,[14] and shows the best cycling performance. As a result, the prepared hierarchically porous carbon materials from silk cocoon are good matrixes for enhancing the utilization rate of sulfur and suppressing the shuttling phenomenon in Li−S batteries.

The rate performance of C-HPCM3200−48.4%S composite cathode was investigated by cycling the cells at various current rates from 0.1 to 1 C. As shown in Figure 9, during the first 12

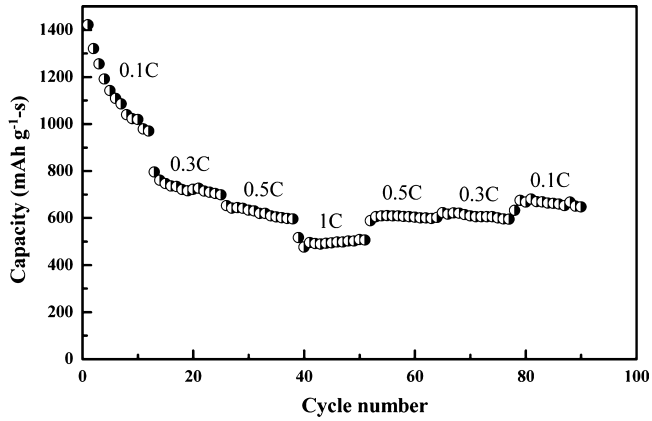

Figure 9. Rate performance of C-HPCM3200−48.4%S composite cathode.

cycles, the discharge capacity decreases gradually at 0.1 *C* rate and remains a capacity of 980 mAh g^{-1}. A capacity of 800 mAh g^{-1} can be delivered at higher rate of 0.3 *C*. When increasing the rate to 0.5 and 1 *C*, reversible capacity of 650 mAh g^{-1} (46% of its initial capacity) and 500 mAh g^{-1} (36% of its initial capacity) are reached, respectively. The cell shows an excellent stability at each rate between 0.3 and 1 *C*. When the charge/discharge rate was changed back to 0.3 and 0.5 *C* in sequence after continuous cycling for 50 times, a capacity almost recovered to its origin one, respectively. When the rate was adjusted back to 0.1 *C* after 80 continuous cycles, a reversible stability of 650 mAh g^{-1} can be restored, demonstrating cyclical stability of C-HPCM/S composite. Presumably, the excellent rate performance of C-HPCM/S composite is due to hierarchical pore structure and good electron conductivity of C-HPCM host matrix.

Figure 10 shows the discharge and charge voltage profiles of C-HPCM-48.4%S composite cathode at a rate of 0.5 C. There are two typical discharge plateaus at about 2.34 and 2.04 V (versus Li/Li^+), which are attributed to the two step reaction of sulfur with Li during the discharge process. As shown in Figure 10, C-HPCM/S composite exhibits good utilization rate of sulfur with an initial discharge capacity of 1335, 1300, and 1250 mAh g^{-1} for the first 3 cycles at a rate of 0.5 *C*. The high initial specific capacity is due to good electron conductivity of C-HPCM host matrix. The initial charge and discharge profiles of C-HPCM/S composites with different sulfur contents are shown in Figure 11. The initial discharge specific capacity decreases along with the increase in sulfur content in C-

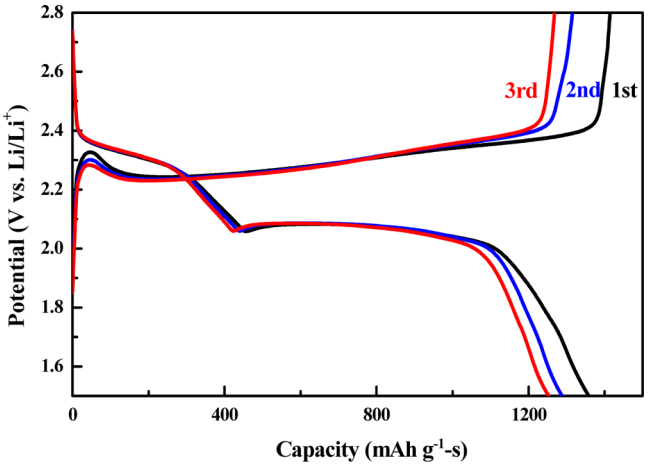

Figure 10. Charge−discharge profiles of C-HPCM3200−48.4%S composite at a rate of 0.5 *C*.

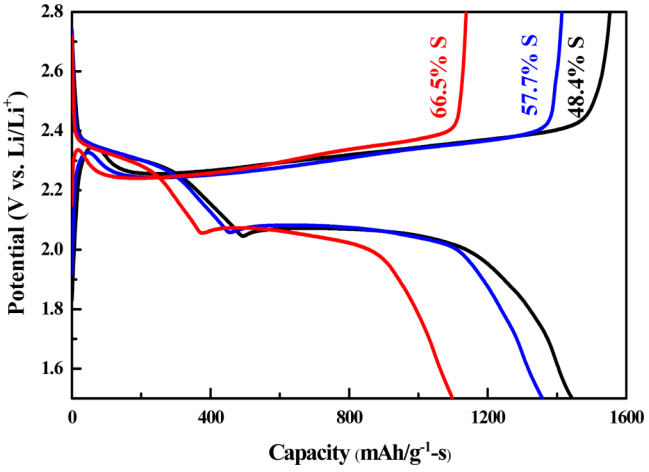

Figure 11. Initial charge−discharge curves of C-HPCM3200/S composites with different sulfur contents at a rate of 0.5 *C*.

HPCM/S composite. C-HPCM3200-48.4%S composite exhibits the highest initial discharge specific capacity. From the results of XRD and SEM measurements, because of the overloading of sulfur, C-HPCM3200-66.5%S composite contained some sulfur on its outer surface that can reduce electron conductivity and lead to its low initial discharge capacity. Furthermore, C-HPCM3200-66.5%S composite shows shorter of discharge plateau than other two composites and exhibits nonpersistent discharge plateaus in the initial discharge curve.

The cyclic voltammogram (CV) curves of C-HPCM-48.4%S composite are shown in Figure 12. Three cycles are scanned continuously in the voltage window of 1.0−3.0 V at scan rate of 0.1 mV s^{-1}. The three curves almost overlap, revealing the steady electrochemical reduction and oxidation reactions. The CV curves shows one oxidation peak (2.33 V versus Li/Li^+) and two reduction peaks (2.34 V, 2.03 V versus Li/Li^+) as the same as the typical CV curves of Li−S batteries. Two reduction peaks are due to the multiple reaction mechanism of sulfur with lithium. The peak at 2.34 V corresponds to the transformation of sulfur to soluble lithium polysulfides (Li_2S_n, $2 < n < 8$), and the peak at 2.03 V associates the reduction of lithium polysulfides to lithium sulfide (Li_2S).[39] The difference between the first reduction peak and the oxidation peak is only 0.1 V in

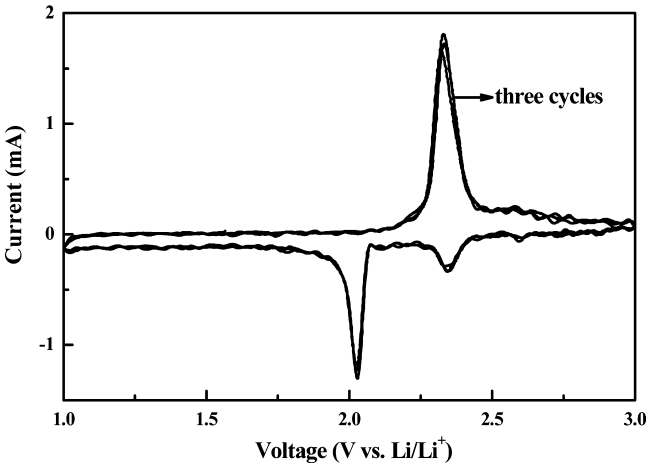

Figure 12. CV curves of C-HPCM3200−48.4%S composite cathode at 0.1 mV s^{-1}.

all CV scans, which indicates the good reversibility of the reaction.[5]

Figure 13 depicts the EIS profiles of C-HPCM/S composite cathodes with different sulfur contents. It can be seen that all

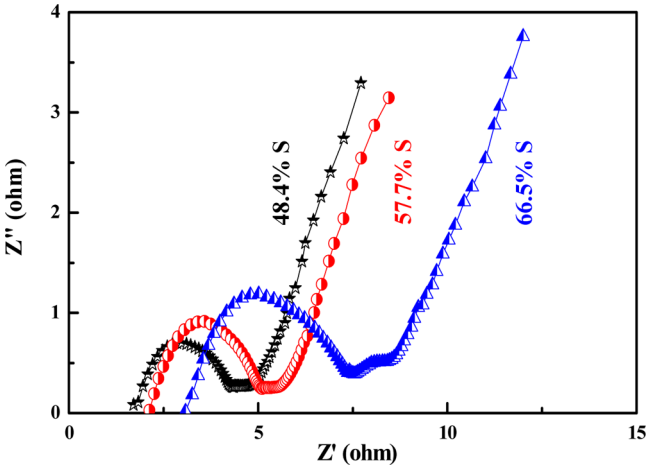

Figure 13. EIS profiles of C-HPCM3200/S composites with different sulfur content between 1 MHz and 0.1 Hz.

Nyquist plots are composed of two depressed semicircles in the middle-high frequency region, and a straight oblique line in the low-frequency region. All C-HPCM/S composites possess similar ohmic resistance (R_o) from the high frequency intercept on the real axis, which are composed of the ionic resistances of the electrolyte, the intrinsic resistance of the active materials and the contact resistance of the interface between the electrodes and current collectors.[40] The semicircle at high-frequency region is attributed to the total resistances of the solid electrolyte interface (SEI) film formed on the electrodes' surface (R_s).[41] Among three C-HPCM/S composites, C-HPCM3200-48.4%S exhibits the lowest R_s, because its low sulfur content and highly conductive porous host matrix facilitate the interface charge and electron transporting.

The semicircle at medium frequency region corresponding to the charge transfer resistance (R_{ct}) is very small for every C-HPCM/S composite, representing the easy charge transporting for electrochemical reactions in the cells. The inclined line at low frequency region corresponds to Warburg impendance

(W_o) for a semi-infinite Warburg diffusion process.[42] The EIS results of C-HPCM/S composites propose that the as prepared C-HPCMs can be used as a good host matrix for Li−S battery applications.

CONCLUSIONS

The hierarchically porous carbon material can be readily prepared by KOH assisted carbonization of silk cocoon biopolymer. A high surface area of 3243 $m^2 g^{-1}$, large pore volume of 2.1 $cm^3 g^{-1}$, and good electron conductivity of 1.0 S cm^{-1} were obtained for C-HPCM3200 carbon material, which was derived from 1:1 weight ratio of precarbonized product to KOH. The as-prepared carbon material can be used as a host matrix for sulfur encapsulation for Li−S battery cathodes. The electrochemical measurements of the composite cathodes in Li−S batteries demonstrate that the hierarchical pores can effectively trap sulfur and the soluble polysulfides intermediates. The highly electron conductive framework can effectively enhance the utilization rate of sulfur. The C-HPCM/S composite with 48.4% sulfur exhibits a very high initial specific capacity of 1443 mAh g^{-1} and retains 804 mAh g^{-1} after 80 cycles, together with a high Coulombic efficiency over 92%. The novel hierarchically porous carbon material from silk cocoon is proven to be a promising carbon matrix for lithium−sulfur battery applications.

AUTHOR INFORMATION

Corresponding Authors

*E-mail: mengyzh@mail.sysu.edu.cn. Fax: 86 20 84114113; Tel: 86 20 84114113.

*E-mail: wangshj@mail.sysu.edu.cn

Notes

The authors declare no competing financial interest.

ACKNOWLEDGMENTS

The authors thank the Link Project of the National Natural Science Foundation of China and Guangdong Province (Grant U1301244); Guangdong Natural Science Foundation (Grant S2012010010545); Guangdong Province Science & Technology Foundation (2011B050300008); Guangdong Province Universities and Colleges Pearl River Scholar Funded Scheme (2010); Guangdong Education Bureau (Key Project: cxzd1004); Chinese Universities Basic Research Founding; "Sino-Greek Science and Technology Cooperation Project (2013DFG2590)" for financial support of this work.

REFERENCES

(1) Zheng, G. Y.; Zhang, Q. F.; Cha, J. J.; Yang, Y.; Li, W. Y.; Seh, Z. W.; Cui, Y. Amphiphilic Surface Modification of Hollow Carbon Nanofibers for Improved Cycle Life of Lithium Sulfur Batteries. *Nano Lett.* **2013**, *13*, 1265−1270.

(2) Lee, J. K.; Kung, M. C.; Trahey, L.; Missaghi, M. N.; Kung, H. H. Nanocomposites Derived from Phenol-Functionalized Si Nanoparticles for High Performance Lithium Ion Battery Anodes. *Chem. Mater.* **2009**, *21*, 6−8.

(3) Whittingham, M. S. Lithium Batteries and Cathode Materials. *Chem. Rev.* **2004**, *104*, 4271−4301.

(4) Armand, M.; Tarascon, J. M. Building Better Batteries. *Nature* **2008**, *451*, 652−657.

(5) Tao, X. Y.; Chen, X. R.; Xia, Y.; Huang, H.; Gan, Y. P.; Wu, R.; Chen, F.; Zhang, W. K. Highly Mesoporous Carbon Foams Synthesized by a Facile, Cost-Effective and Template-Free Pechini Method for Advanced Lithium−Sulfur Batteries. *J. Mater. Chem. A* **2013**, *1*, 3295−3301.

(6) Zhao, S. R.; Li, C. M.; Wang, W. K.; Zhang, H.; Gao, M. Y.; Xiong, X.; Wang, A. B.; Yuan, K. G.; Huang, Y. Q.; Wang, F. A Novel Porous Nanocomposite of Sulfur/Carbon Obtained from Fish Scales for Lithium−Sulfur Batteries. *J. Mater. Chem. A* **2013**, *1*, 3334−3339.

(7) Wang, H. L.; Yang, Y.; Liang, Y. Y.; Robinson, J. T.; Li, Y. G.; Jackson, A.; Cui, Y.; Dai, H. J. Graphene-Wrapped Sulfur Particles as a Rechargeable Lithium-Sulfur Battery Cathode Material with High Capacity and Cycling Stability. *Nano Lett.* **2011**, *11*, 2644−2647.

(8) Liang, C.; Dudney, N. J.; Howe, J. Y. Hierarchically Structured Sulfur/Carbon Nanocomposite Material for High-Energy Lithium Battery. *Chem. Mater.* **2009**, *21*, 4724−4730.

(9) Marmorstein, D.; Yu, T. H.; Striebel, K. A.; McLarnon, F. R.; Hou, J.; Cairns, E. J. Electrochemical Performance of Lithium Sulfur Cells with Three Different Polymer Electrolytes. *J. Power Sources* **2000**, *89*, 219−226.

(10) Bruce, P. G.; Freunberger, S. A.; Hardwick, L. J.; Tarascon, J. M. Li−O_2 and Li−S Batteries with High Energy Storage. *Nat. Mater.* **2012**, *11*, 19−29.

(11) Ji, X. L.; Nazar, L. F. Advances in Li−S Batteries. *J. Mater. Chem.* **2010**, *20*, 9821−9826.

(12) Chung, W. J.; Griebel, J. J.; Kim, E. T.; Yoon, H.; Simmonds, A. G.; Ji, H. J.; Dirlam, P. T.; Glass, R. S.; Wie, J. J.; Nguyen, N. A.; Guralnick, B. W.; Park, J.; Somogyi, Á.; Theato, P.; Mackay, M. E.; Sung, Y. E.; Char, K.; Pyun, J. The Use of Elemental Sulfur as an Alternative Feedstock for Polymeric Materials. *Nat. Chem.* **2013**, *5*, 518−524.

(13) Wang, Y. X.; Huang, L.; Sun, L. C.; Xie, S. Y.; Xu, G. L.; Chen, S. R.; Xu, Y. F.; Li, J. T.; Chou, S. L.; Dou, S. X.; Sun, S. G. Facile Synthesis of a Interleaved Expanded Graphite-Embedded Sulphur Nanocomposite as Cathode of Li−S Batteries with Excellent Lithium Storage Performance. *J. Mater. Chem.* **2012**, *22*, 4744−4750.

(14) Ji, X.; Lee, K. T.; Nazar, L. F. A Highly Ordered Nanostructured Carbon−Sulphur Cathode for Lithium−Sulphur Batteries. *Nat. Mater.* **2009**, *8*, 500−506.

(15) Wang, J.; Lu, L.; Choucair, M.; Stride, J. A.; Xu, X.; Liu, H. Sulfur-Graphene Composite for Rechargeable Lithium Batteries. *J. Power Sources* **2011**, *196*, 7030−7034.

(16) Mikhaylik, Y. V.; Akridge, J. R. Polysulfide Shuttle Study in the Li/S Battery System. *J. Electrochem. Soc.* **2004**, *151*, A1969−A1976.

(17) Seh, Z. W.; Li, W. Y.; Cha, J. J.; Zheng, G. Y.; Yang, Y.; McDowell1, M. T.; Hsu, P. C.; Cui, Y. Sulphur-TiO_2 Yolk-Shell Nanoarchitecture with Internal Void Space for Long-Cycle Lithium-Sulphur Batteries. *Nat. Commun.* **2013**, *4*, 1331.

(18) Su, Y. S.; Fu, Y. Z.; Manthiram, A. Self-Weaving Sulfur−Carbon Composite Cathodes for High Rate Lithium-Sulfur Batteries. *Phys. Chem. Chem. Phys.* **2012**, *14*, 14495−14499.

(19) Xu, G. Y.; Ding, B.; Shen, L. F.; Nie, P.; Han, J. P.; Zhang, X. G. Sulfur Embedded in Metal Organic Framework-Derived Hierarchically Porous Carbon Nanoplates for High Performance Lithium−Sulfur Battery. *J. Mater. Chem. A* **2013**, *1*, 4490−4496.

(20) Xi, K.; Cao, S.; Peng, X. Y.; Ducati, C.; Kumar, R. V.; Cheetham, A. K. Carbon with Hierarchical Pores from Carbonized Metal−Organic Frameworks for Lithium Sulphur Batteries. *Chem. Commun.* **2013**, *49*, 2192−2194.

(21) Fanous, J.; Wegner, M.; Grimminger, J.; Andresen, Ä.; Buchmeiser, M. R. Structure-Related Electrochemistry of Sulfur-Poly(acrylonitrile) Composite Cathode Materials for Rechargeable Lithium Batteries. *Chem. Mater.* **2011**, *23*, 5024−5028.

(22) Trofimov, B. A.; Myachina, G. F.; Rodionova, I. V.; Mal'kina, A. G.; Dorofeev, I. A.; Vakul'skaya, T. I.; Sinegovskaya, L. M.; Skotheim, T. A. Ethynedithiol-Based Polyeneoligosulfides as Active Cathode Materials for Lithium-Sulfur Batteries. *J. Appl. Polym. Sci.* **2008**, *107*, 784−787.

(23) Wang, J.; Chen, J.; Konstantinov, K.; Zhao, L.; Ng, S. H.; Wang, G. X.; Guo, Z. P.; Liu, H. K. Sulphur-Polypyrrole Composite Positive Electrode Materials for Rechargeable Lithium Batteries. *Electrochim. Acta* **2006**, *51*, 4634−4638.

(24) Wang, J.; Yang, J.; Xie, J.; Xu, N. A Novel Conductive Polymer-Sulfur Composite Cathode Material for Rechargeable Lithium Batteries. *Adv. Mater.* **2002**, *14*, 963−965.
(25) Wu, F.; Wu, S. X.; Chen, R. J.; Chen, J. Z.; Chen, S. Sulfur−Polythiophene Composite Cathode Materials for Rechargeable Lithium Batteries. *Electrochem. Solid-State Lett.* **2010**, *13*, A29−A31.
(26) Schuster, J.; He, G.; Mandlmeier, B.; Yim, T.; Lee, K. T.; Bein, T.; Nazar, L. F. Spherical Ordered Mesoporous Carbon Nanoparticles with High Porosity for Lithium−Sulfur Batteries. *Angew. Chem., Int. Ed.* **2012**, *51*, 3591−3595.
(27) Xiao, M.; Huang, M.; Zeng, S. S.; Han, D. M.; Wang, S. J.; Sun, L. Y.; Meng, Y. Z. Sulfur@Graphene Oxide Core−Shell Particles as a Rechargeable Lithium−Sulfur Battery Cathode Material with High Cycling Stability and Capacity. *RSC Adv.* **2013**, *3*, 4914−4916.
(28) Han, S. C.; Song, M. S.; Lee, H.; Kim, H. S.; Ahn, H. J.; Lee, J. Y. Effect of Multiwalled Carbon Nanotubes on Electrochemical Properties of Lithium/Sulfur Rechargeable Batteries. *J. Electrochem. Soc.* **2003**, *150*, A889−A893.
(29) Oschatz, M.; Thieme, S.; Borchardt, L.; Lohe, M. R.; Biemelt, T.; Brückner, J.; Althues, H.; Kaskel, S. A New Route for the Preparation of Mesoporous Carbon Materials with High Performance in Lithium−Sulphur Battery Cathodes. *Chem. Commun.* **2013**, *49*, 5832−5834.
(30) Liang, Y. R.; Wu, D. C.; Fu, R. W. Carbon Microfibers with Hierarchical Porous Structure from Electrospun Fiber-Like Natural Biopolymer. *Sci. Rep.* **2013**, *3*, 1119.
(31) Yun, Y. S.; Cho, S. Y.; Shim, J. Y.; Kim, B. H.; Chang, S. J.; Baek, S. J.; Huh, Y. S.; Tak, Y.; Park, Y. W.; Park, S. J.; Jin, H. J. Microporous Carbon Nanoplates from Regenerated Silk Proteins for Supercapacitors. *Adv. Mater.* **2013**, *25*, 1993−1998.
(32) Piñero, E. R.; Azaïs, P.; Cacciaguerra, T.; Amorós, D. C.; Solano, A. L.; Béguin, F. KOH and NaOH Activation Mechanisms of Multiwalled Carbon Nanotubes with Different Structural Organisation. *Carbon* **2005**, *43*, 786−795.
(33) Sun, X.; Wang, X.; Mayes, R. T.; Dai, S. Lithium−Sulfur Batteries Based on Nitrogen-Doped Carbon and an Ionic-Liquid Electrolyte. *ChemSusChem* **2012**, *5*, 2079−2085.
(34) Sun, F. G.; Wang, J. T.; Chen, H. C.; Li, W. C.; Qiao, W. M.; Long, D. H.; Ling, L. C. High Efficiency Immobilization of Sulfur on Nitrogen-Enriched Mesoporous Carbons for Li−S Batteries. *ACS Appl. Mater. Interfaces* **2013**, *5*, 5630−5638.
(35) Li, D.; Han, F.; Wang, S.; Cheng, F.; Sun, Q.; Li, W. C. High Sulfur Loading Cathodes Fabricated Using Peapodlike, Large Pore Volume Mesoporous Carbon for Lithium−Sulfur Battery. *ACS Appl. Mater. Interfaces* **2013**, *5*, 2208−2213.
(36) Yu, L. H.; Brun, N.; Sakaushi, K.; Eckert, J.; Titirici, M. M. Hydrothermal Nanocasting: Synthesis of Hierarchically Porous Carbon Monoliths and Their Application in Lithium−Sulfur Batteries. *Carbon* **2013**, *61*, 245−253.
(37) Li, G. C.; Hu, J. J.; Li, G. R.; Ye, S. H.; Gao, X. P. Sulfur/Activated-Conductive Carbon Black Composites as Cathode Materials for Lithium/Sulfur Battery. *J. Power Sources* **2013**, *240*, 598−605.
(38) Cakan, R. D.; Morcrette, M.; Gangulibabu; Guéguen, A.; Dedryvère, R.; Tarascon, J. M. Li−S Batteries: Simple Approaches for Superior Performance. *Energy Environ. Sci.* **2013**, *6*, 176−182.
(39) Zhou, G. M.; Wang, D. W.; Li, F.; Hou, P. X.; Yin, L. C.; Liu, C.; Lu, G. Q.; Gentle, I. R.; Cheng, H. M. A Flexible Nanostructured Sulphur−Carbon Nanotube Cathode with High Rate Performance for Li-S Batteries. *Energy Environ. Sci.* **2012**, *5*, 8901−8906.
(40) Canas, N. A.; Hirose, K.; Pascucci, B.; Wagner, N.; Friedrich, K. A.; Hiesgen, R. Investigations of Lithium−Sulfur Batteries Using Electrochemical Impedance Spectroscopy. *Electrochim. Acta* **2013**, *97*, 42−51.
(41) Deng, Z. F.; Zhang, Z. A.; Lai, Y. Q.; Liu, J.; Li, J.; Liu, Y. X. Electrochemical Impedance Spectroscopy Study of a Lithium/Sulfur Battery: Modeling and Analysis of Capacity Fading. *J. Electrochem. Soc.* **2013**, *160*, A553−A558.
(42) Ding, B.; Shen, L. F.; Xu, G. Y.; Nie, P.; Zhang, X. G. Encapsulating Sulfur into Mesoporous TiO_2 Host as a High Performance Cathode for Lithium−Sulfur Battery. *Electrochim. Acta* **2013**, *107*, 78−84.